

Transport and mixing in the extratropical tropopause region in a high vertical resolution GCM

(Miyazaki et al. JAS 2010a,2010b)

Kazuyuki Miyazaki

Royal Netherlands Meteorological Institute (KNMI)



Japan Agency for Marine-Earth Science and Technology (JAMSTEC)



Kaoru Sato: *University of Tokyo*

Shingo Watanabe: *JAMSTEC*

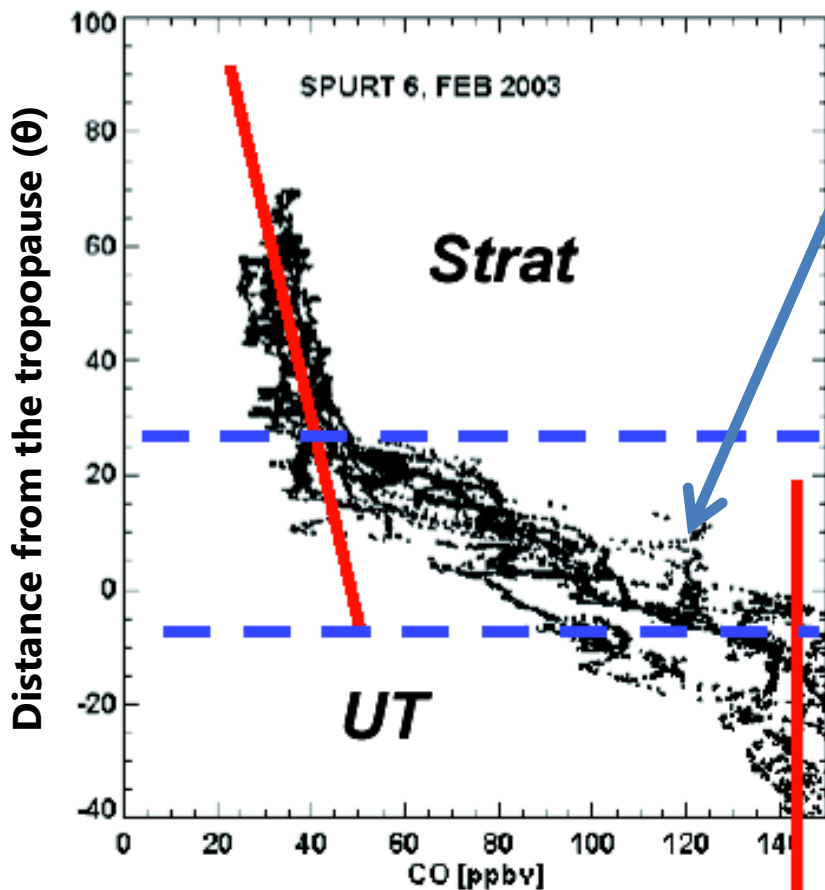
Yoshihiro Tomikawa: *NIPR*

Yoshio Kawatani: *JAMSTEC*



Masaaki Takahashi *University of Tokyo*

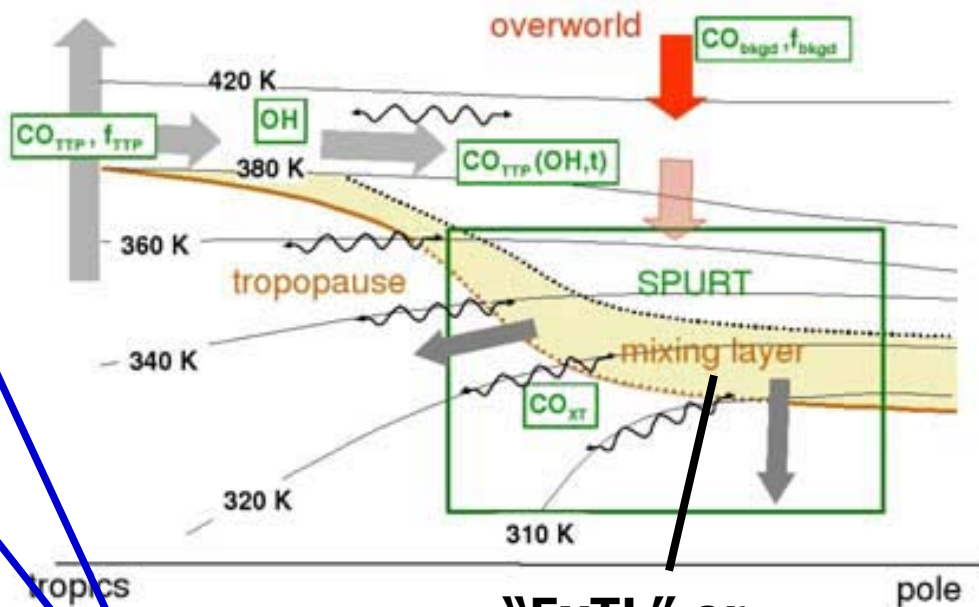
Extratropical tropopause transition layer (ExTL)



CO profiles as a function of a distance from the tropopause

Transition layer
(thickness = 2 km)

(Hoor et al., 2004)

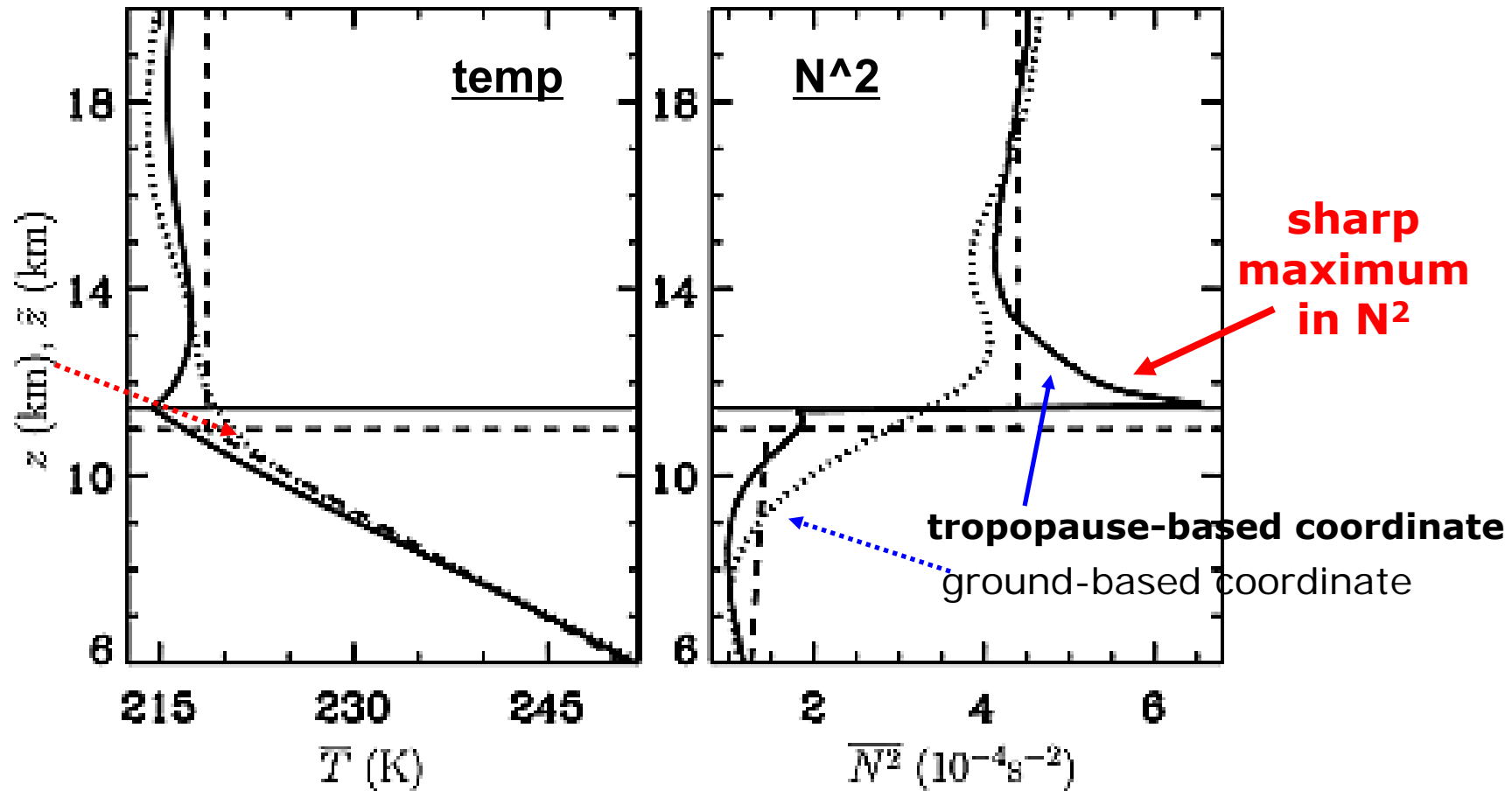


“ExTL” or
“Tropopause mixing layer”

Transport barrier?

Chemical tracers have intermediate concentrations in the extratropical tropopause region.

Tropopause inversion layer (TIL)



(Birner et al., 2006; Randel et al., 2007)

A large temperature gradient in the lowermost stratosphere forms a tropopause inversion layer (TIL) just above the extratropical tropopause

-The similar locations of the TIL and ExTL imply that the chemical and thermal structures interact with each other in the extratropical tropopause region (e.g., Randel et al., 2007).

- relationship between the mechanisms of formation of the TIL and the ExTL ?

- relative importance of transport processes at different scales ?

- current models do not fully succeed in simulating the location and depth of these layers (e.g., CCMval inter-comparisons).

KANTO project: A high vertical resolution GCM

T213L256 GCM:

vertical resolution = 300 m, top=85km

horizontal resolution = 0.5625°

No gravity wave drag parameterization

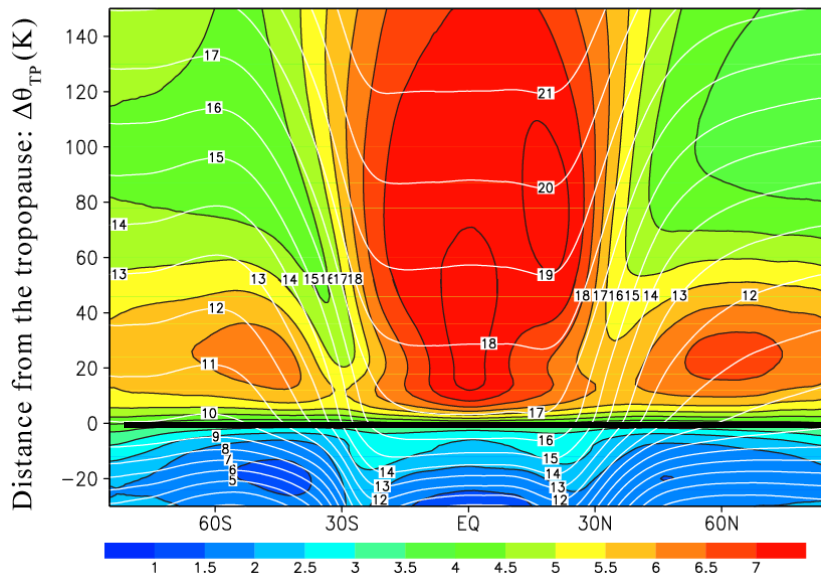
Watanabe et al., JGR2008, JGR2009, Tomikawa et al., JGR2008,
Kawatani et al., JAS2010a & JAS2010b, Sato et al., GRL2009,
Miyazaki et al., JAS2010a & JAS2010b

- **gravity wave propagations and the induced circulation**
- **fine thermal/dynamical structure around the tropopause**
- **importance of variously scaled atmospheric processes**

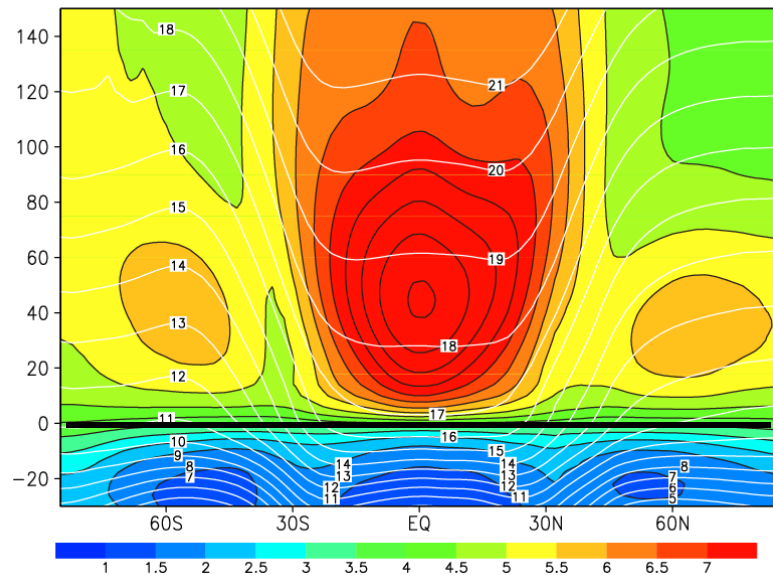
Comparisons with a coarse-resolution GCM ($\Delta z \approx 1\text{km}$)

N^2

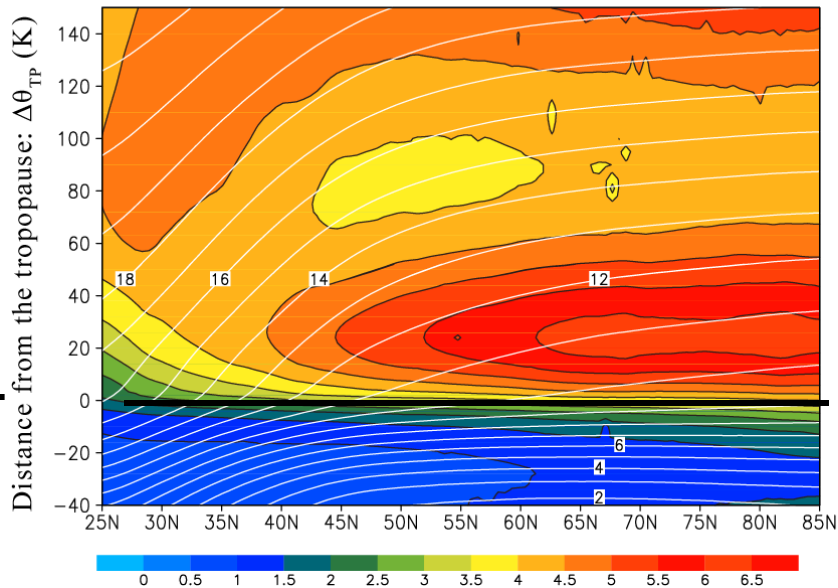
(a) N^2 : T213L256



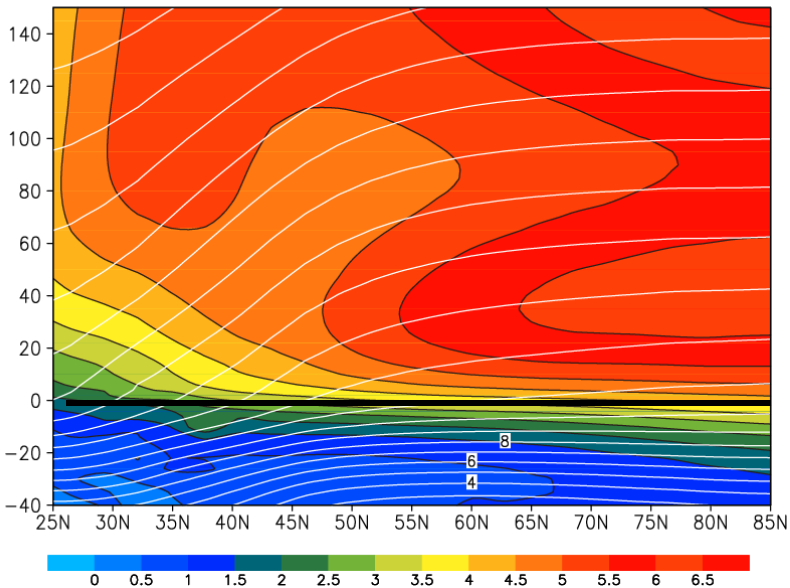
(b) N^2 : T42L32



(c) MPV: T213L256



(d) MPV: T42L32

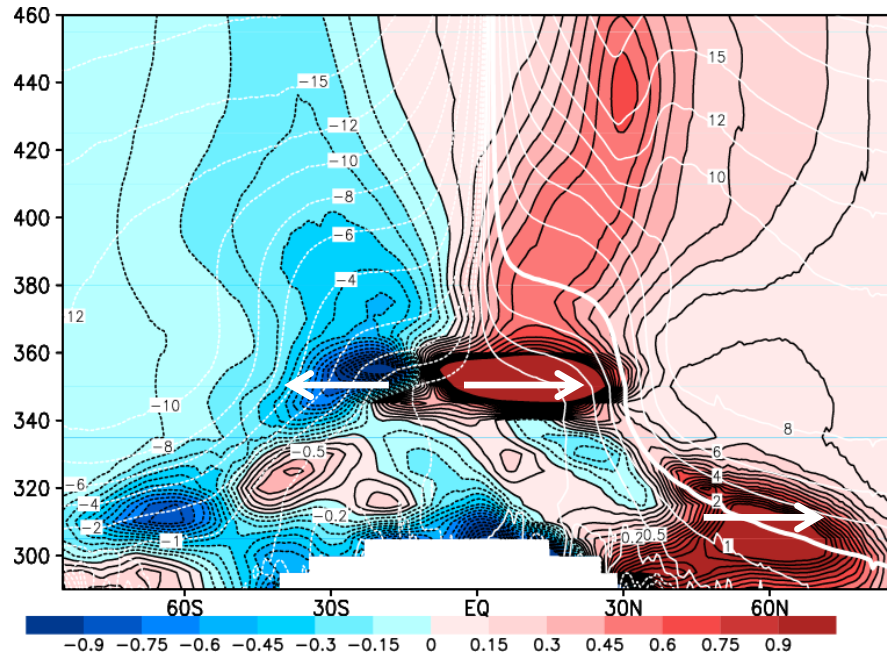


θ
tropopause
based-coord.

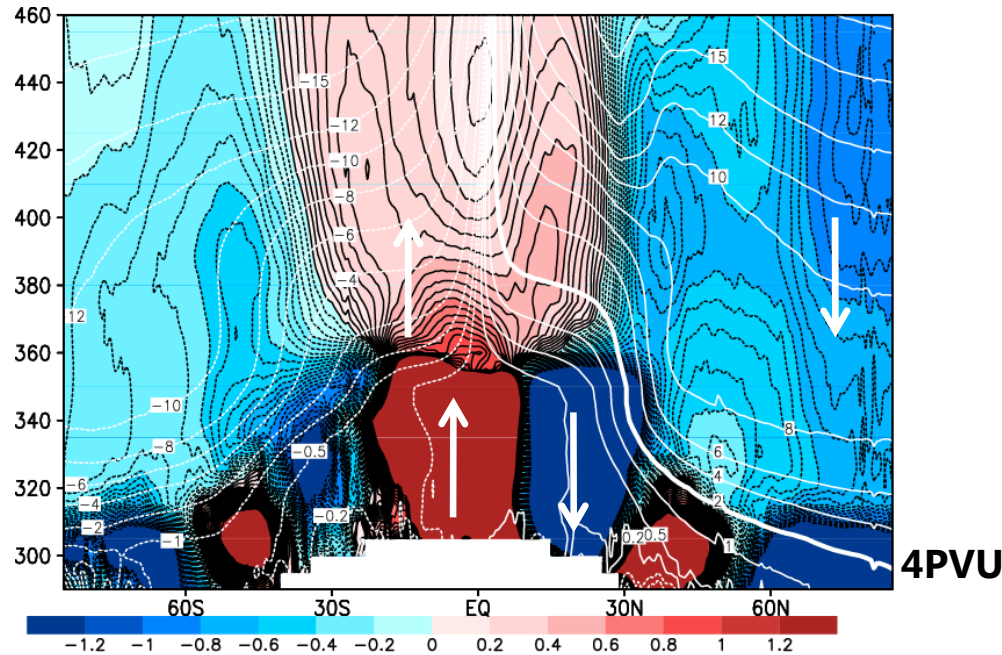
Lat.

Mean-meridional circulation January

Mean meridional wind V^*



Mean vertical wind W^*



Compared to coarse resolution models:

- stronger convergence of the mean downward velocity in the LS
- stronger and sharper meridional divergent flows in the UT

The PV is a material invariant (i.e., passive tracer) under inviscid (frictionless) and adiabatic approximation (Hoskins, 1985).

Continuity equation of isentropic PV;

$$\frac{D_{\theta}q}{Dt} = \frac{\partial q}{\partial t} + \vec{v} \cdot \nabla_{\theta} q = \frac{q}{\sigma} \frac{\partial}{\partial \theta} (\sigma \dot{\theta}) + \sigma^{-1} \vec{k} \cdot \nabla_{\theta} \times \left(\vec{F}_r - \dot{\theta} \frac{\partial \vec{v}}{\partial \theta} \right)$$

Zonal mean equation based on the mass-weighted isentropic zonal means

$$\frac{\partial \overline{q^*}}{\partial t} = -\frac{\overline{v^*} \partial \overline{q^*}}{a \partial \phi} - \frac{\overline{\dot{\theta}^*} \partial \overline{q^*}}{\partial \theta} - \frac{1}{a \cos \phi} \frac{\partial (\overline{v'q'})^* \cos \phi}{\partial \phi} - \frac{1}{\rho_0} \frac{\partial \rho_0 (\overline{\dot{\theta}'q'})^*}{\partial z_{\dagger}} + \left(\overline{q \frac{\partial \dot{\theta}}{\partial \theta}} \right)^*$$

If the source/sink effect is negligible, this analysis provides insights into transport processes related to formation of long-lived tracer concentration gradients

Analysis of maintain mechanisms of vertical PV gradients

$$\begin{aligned} \frac{\partial}{\partial t} \left(\frac{\partial \overline{q^*}}{\partial \theta} \right) &= \underbrace{-\frac{\partial \overline{q^*} \partial \overline{v^*}}{a \partial \phi \partial \theta}}_{MEY1} - \underbrace{\overline{v^*} \frac{\partial^2 \overline{q^*}}{a \partial \phi \partial \theta}}_{MEY2} - \underbrace{\frac{\partial \overline{\dot{\theta}^*} \partial \overline{q^*}}{\partial \theta \partial \theta}}_{MEZ1} - \underbrace{\overline{\dot{\theta}^*} \frac{\partial^2 \overline{q^*}}{\partial \theta^2}}_{MEZ2} \\ &- \underbrace{\frac{\partial}{\partial \theta} \left(-\frac{1}{a \cos \phi} \frac{\partial (\overline{v'q'})^* \cos \phi}{\partial \phi} \right)}_{EDY} - \underbrace{\frac{\partial}{\partial \theta} \left(\frac{1}{\rho_0} \frac{\partial \rho_0 (\overline{\dot{\theta}'q'})^*}{\partial \theta} \right)}_{EDZ} + \underbrace{\frac{\partial}{\partial \theta} \left(\overline{q \frac{\partial \dot{\theta}}{\partial \theta}} \right)^*}_{source/sink} \end{aligned}$$

Maintain mechanisms of PV gradients

$$\frac{\partial}{\partial t} \left(\frac{\partial \bar{q}^*}{\partial \theta} \right) = \underbrace{-\frac{\partial \bar{q}^*}{a \partial \phi} \frac{\partial \bar{v}^*}{\partial \theta}}_{MEY1} - \underbrace{\bar{v}^* \frac{\partial^2 \bar{q}^*}{a \partial \phi \partial \theta}}_{MEY2} + \underbrace{\frac{\partial \bar{\theta}^*}{\partial \theta} \frac{\partial \bar{q}^*}{\partial \theta}}_{MEZ1} + \underbrace{\bar{\theta}^* \frac{\partial^2 \bar{q}^*}{\partial \theta^2}}_{MEZ2} + \text{EDY} + \text{EDZ} + \text{source}$$

January

July

(a) Mean meridional (MEY1): JAN

(b) Mean meridional (MEY2): JAN

(a) Mean meridional (MEY1): JUL

(b) Mean meridional (MEY2): JUL

Winter: mean downward transport and isentropic mixing

Summer: mean downward transport and vertical mixing

Distance from the tropopause: $\Delta \theta_{TP}$ (K)

(c) Mean vertical (MEZ1): JAN

(d) Mean vertical (MEZ2): JAN

(c) Mean vertical (MEZ1): JUL

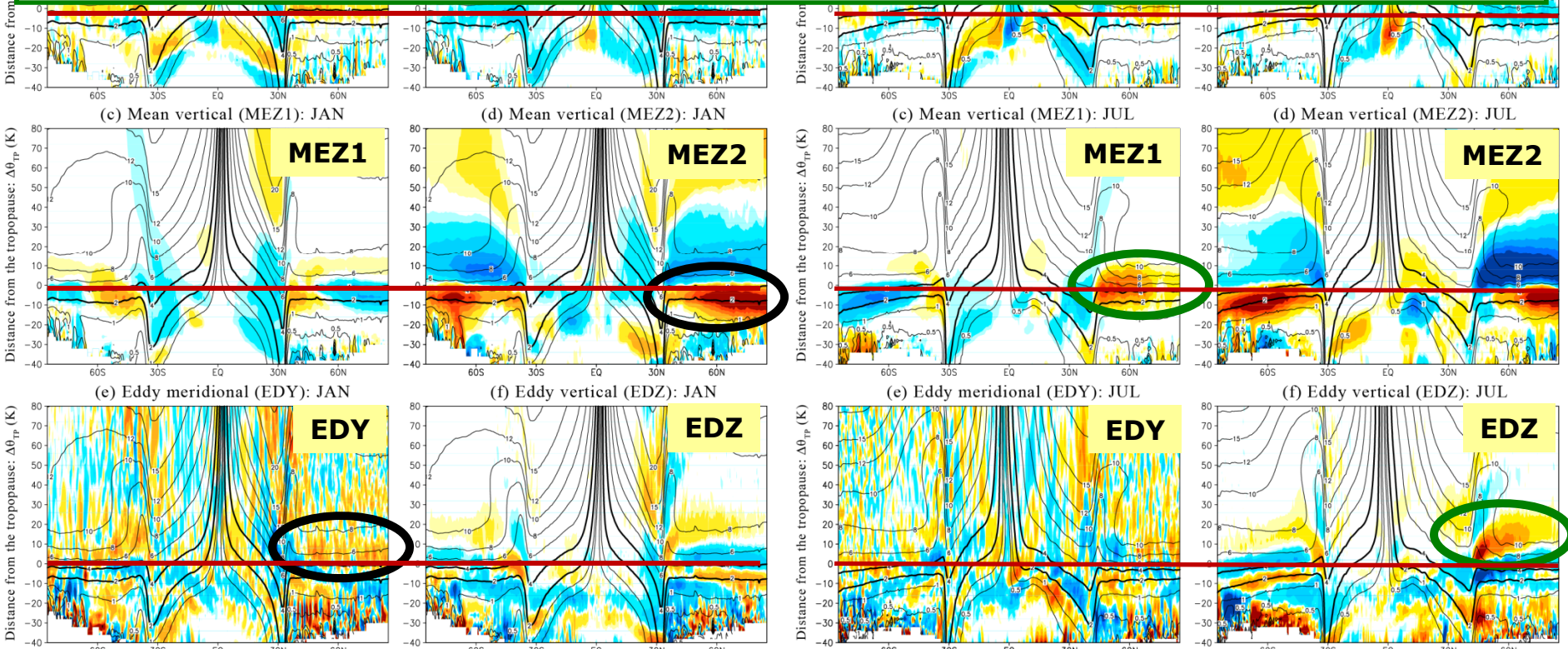
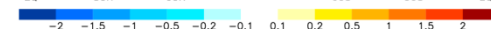
(d) Mean vertical (MEZ2): JUL

(e) Eddy meridional (EDY): JAN

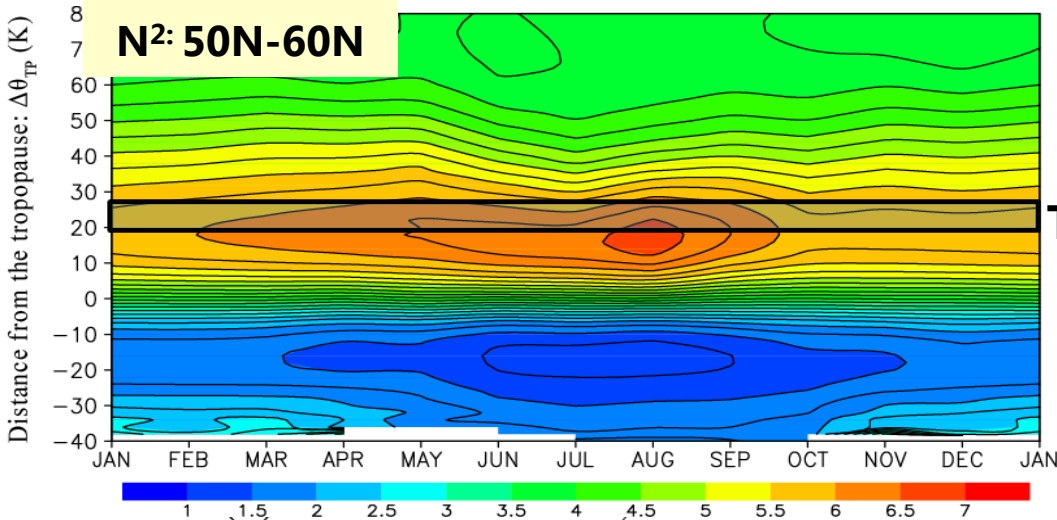
(f) Eddy vertical (EDZ): JAN

(e) Eddy meridional (EDY): JUL

(f) Eddy vertical (EDZ): JUL

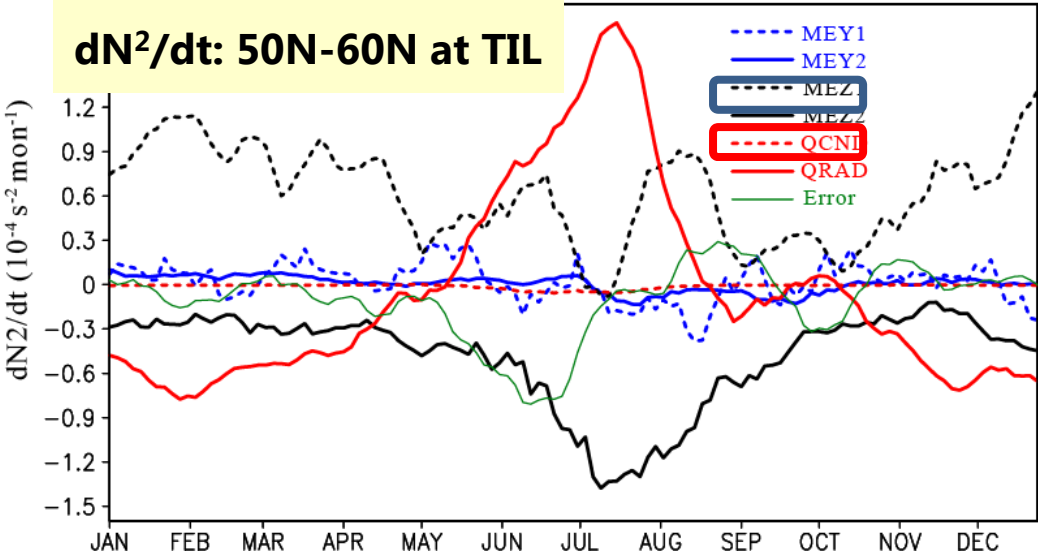


TIL formation mechanisms



TIL

-Stratification by radiation and downward advection of the static stability profile determine seasonal variation of the TIL.



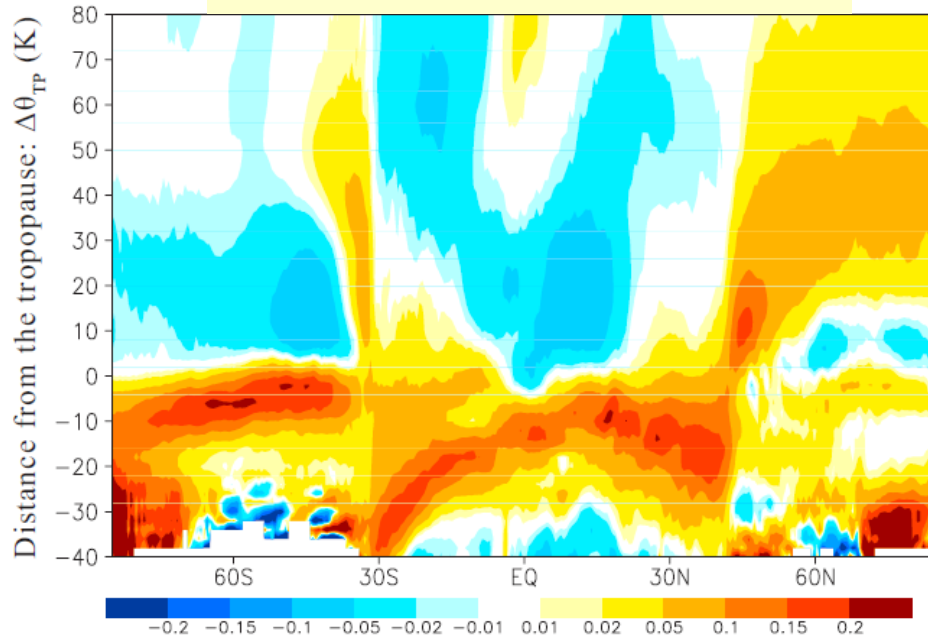
- Radiation -> summertime maximum

Thermodynamic analysis

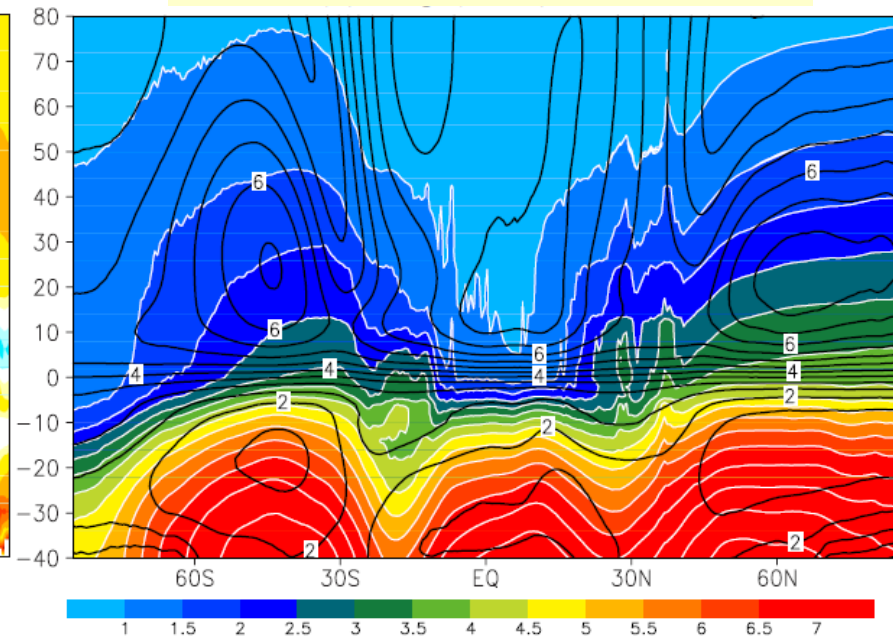
$$\frac{\partial \overline{N^2}}{\partial t} = \left(\underbrace{\frac{\overline{v^*}}{\partial z_{\dagger}} \frac{\partial \theta}{\partial \phi}}_{MEY1} \underbrace{- \frac{\overline{v^*}}{a \partial \phi \partial z_{\dagger}} \frac{\partial^2 \theta}{\partial z_{\dagger}^2}}_{MEY2} \underbrace{- \frac{\partial \overline{w_{\dagger}^*}}{\partial z_{\dagger}} \frac{\partial \theta}{\partial z_{\dagger}}}_{MEZ1} \underbrace{- \frac{\overline{w_{\dagger}^*}}{\partial z_{\dagger}} \frac{\partial^2 \theta}{\partial z_{\dagger}^2}}_{MEZ2} \underbrace{+ \frac{\partial \overline{Q_{rad}^*}}{\partial z_{\dagger}}}_{QRAD} \underbrace{+ \frac{\partial \overline{Q_{cnd}^*}}{\partial z_{\dagger}}}_{QCND} \right) / \left(\frac{\theta}{g} \right)$$

July

dN^2/dt by radiation



Log(H₂O)



- ExTL and TIL can have similar locations, as a result of common dynamic processes and interactions between constituent distributions and thermal structure

-downward advection of constituents and heat at the lower part
-eddy mixing (suppression) of constituents (e.g., H₂O) and radiative stratification at the upper part

Downward control

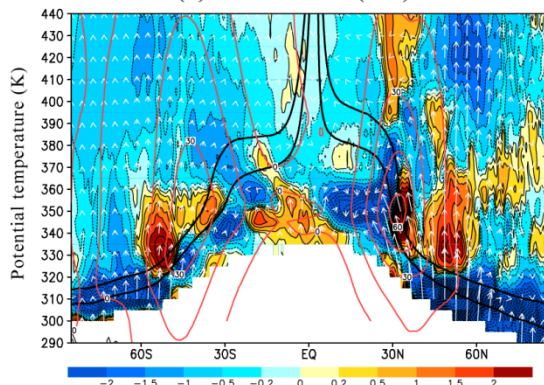
PW: n=1-3

MW: n=4-20

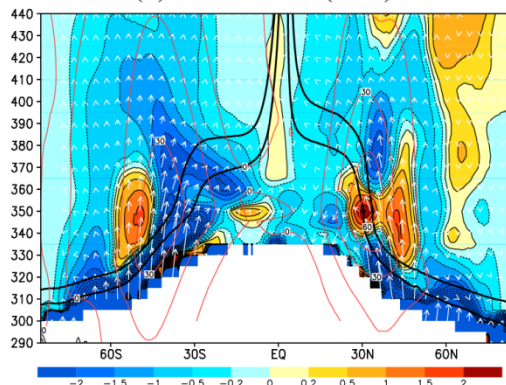
GW: n=21-

Div.
EP-F

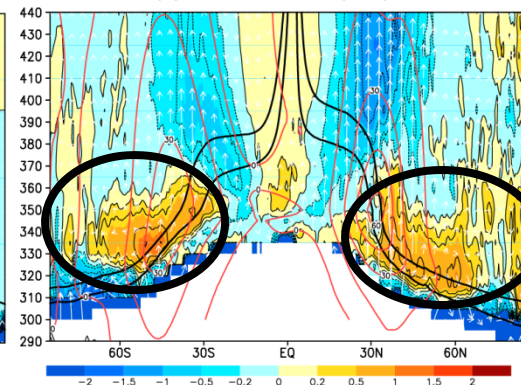
(a) EP-flux: PW(1-3)



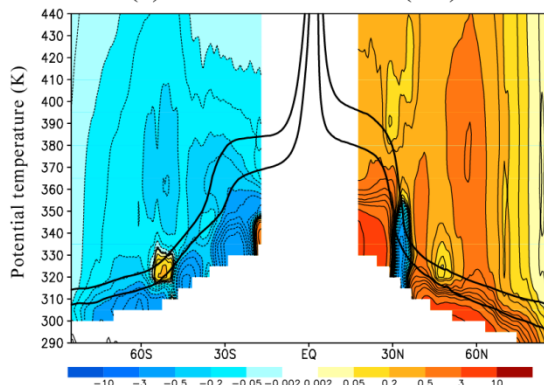
(b) EP-flux: MW(4-20)



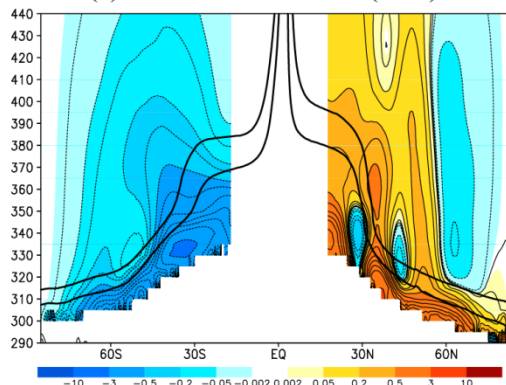
(c) EP-flux: GW(21-)



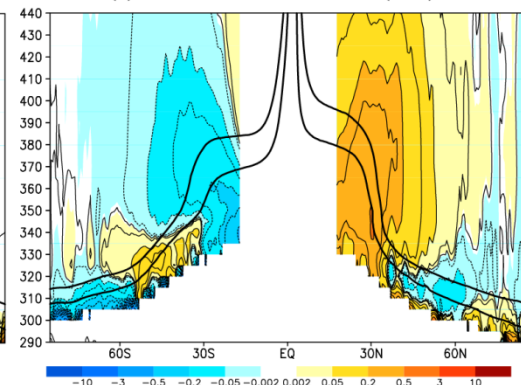
(d) Stream function: PW(1-3)



(e) Stream function: MW(4-20)



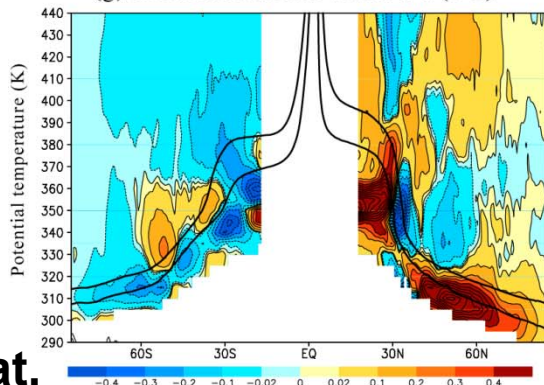
(f) Stream function: GW(21-)



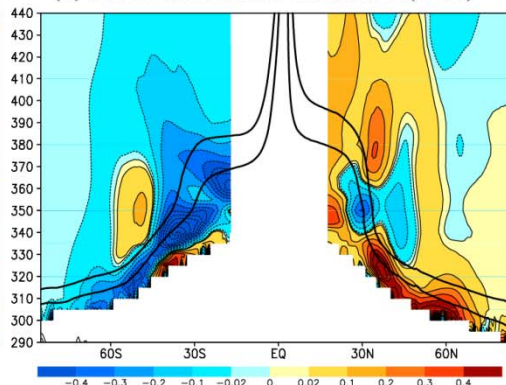
Stream
func.

January

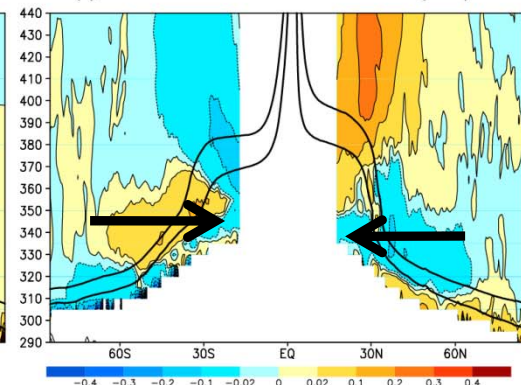
(g) Mean meridional wind: PW(1-3)



(h) Mean meridional wind: MW(4-20)



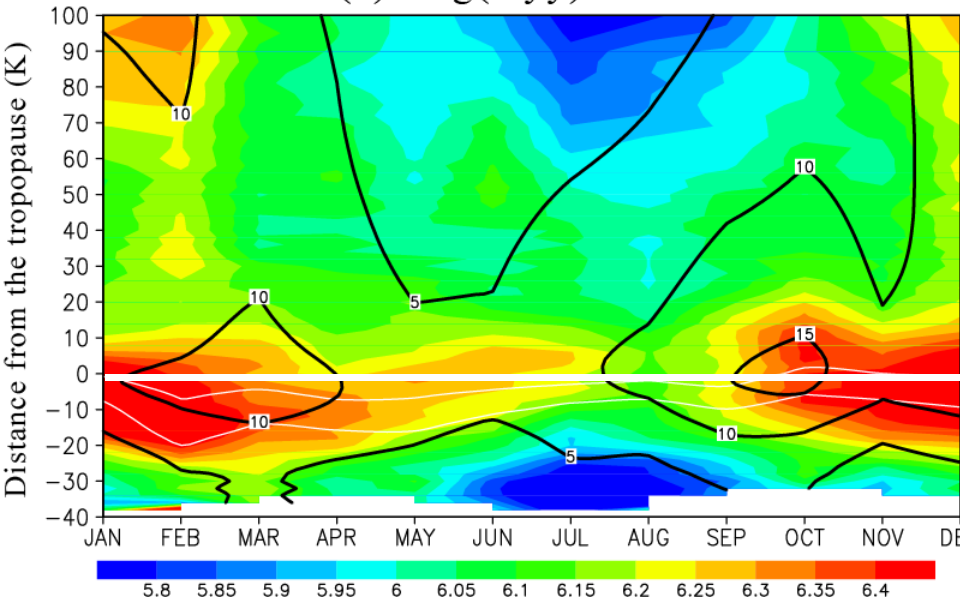
(i) Mean meridional wind: GW(21-)



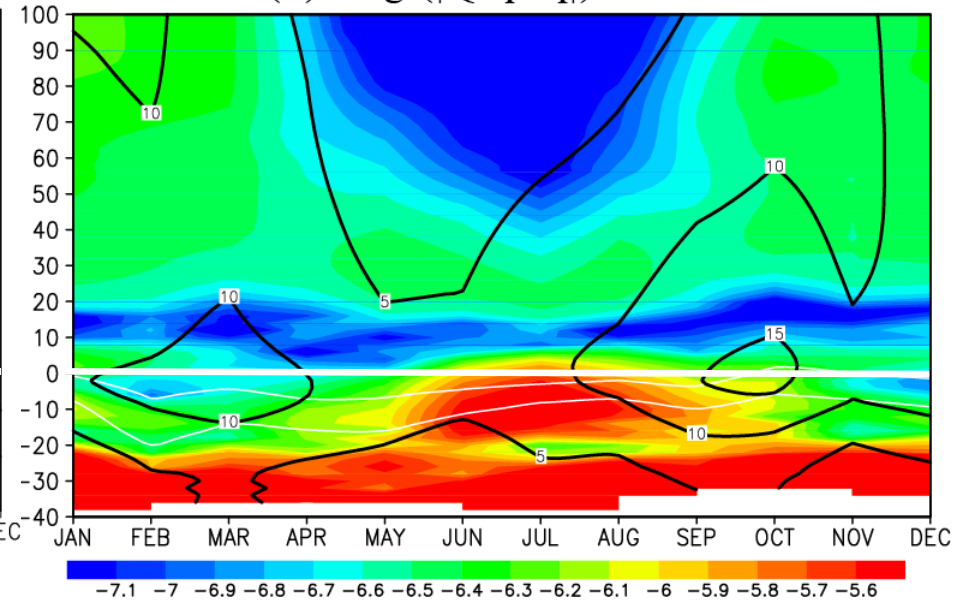
θ
 V^*
Lat.

Seasonal variation of horizontal and vertical mixing

(a) Log(K_{yy}): 60N



(b) Log ($|Q'q'/\bar{q}|$): 60N



**Horizontal
diffusion
coefficient**

$$\left[\overline{(v'q')^*} \right]_t \simeq -K_{yy}(t) \left[\left(\frac{\partial \bar{q}^*}{\partial \phi} \right)_{\theta} \right]_t$$

**Vertical
diffusion** $\left| \frac{\overline{Q'q'}}{\bar{q}} \right|$

- Strong isentropic mixing between 20 K below-10 K above the tropopause
- Vertical eddy mixing is substantial in the tropopause region during summer, but is strongly suppressed just above the well-mixed region

50N-60N January

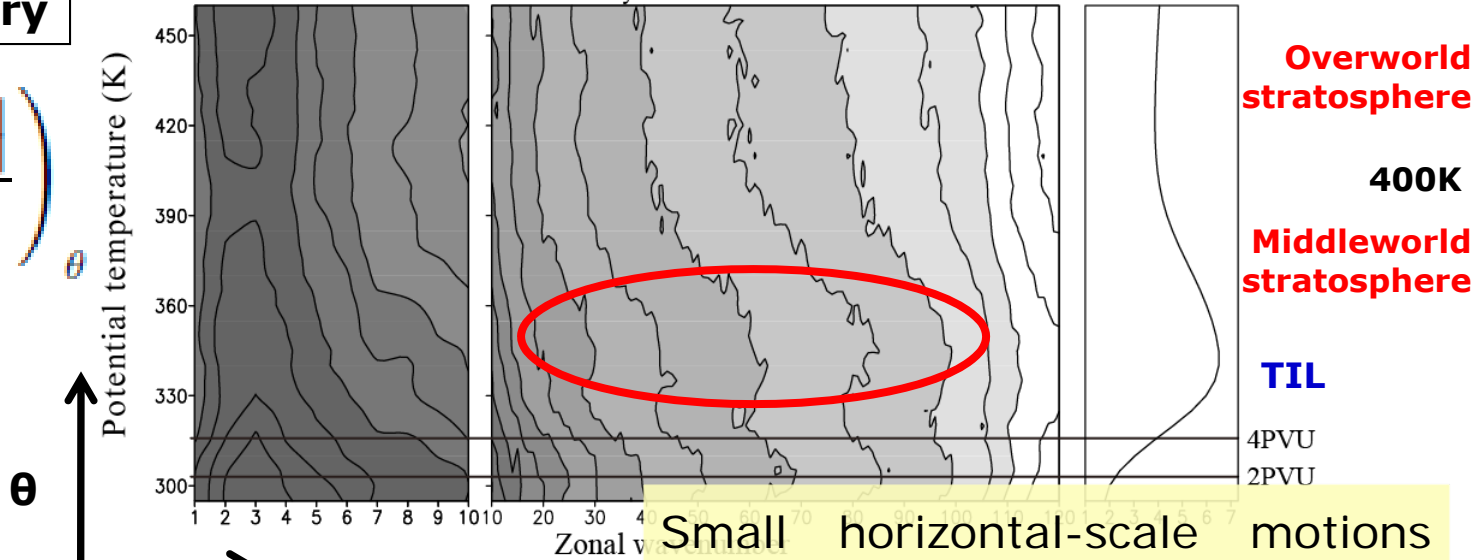
$$K_{yy(s)} = \left(\frac{|v'_s q'_s|}{\frac{\partial q^*}{\partial \phi}} \right) \theta$$

Isentropic mixing

Zonal wave number (s)

Log[|v'_s q'_s|/(q_y)]: 50N-60N JAN

N²



Overworld stratosphere

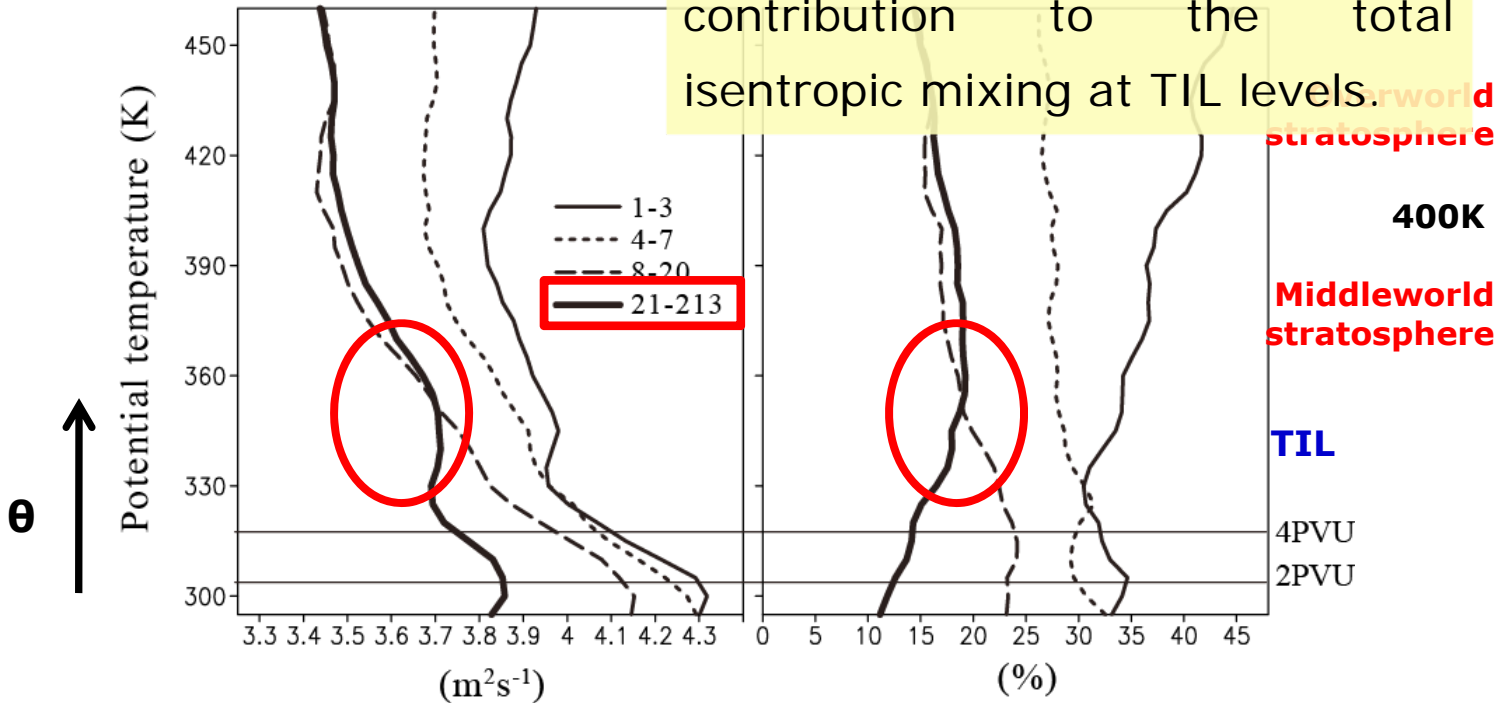
400K

Middleworld stratosphere

TIL

4PVU
2PVU

Small horizontal-scale motions (s > 21) provide an important contribution to the total isentropic mixing at TIL levels.



Overworld stratosphere

400K

Middleworld stratosphere

TIL

4PVU
2PVU

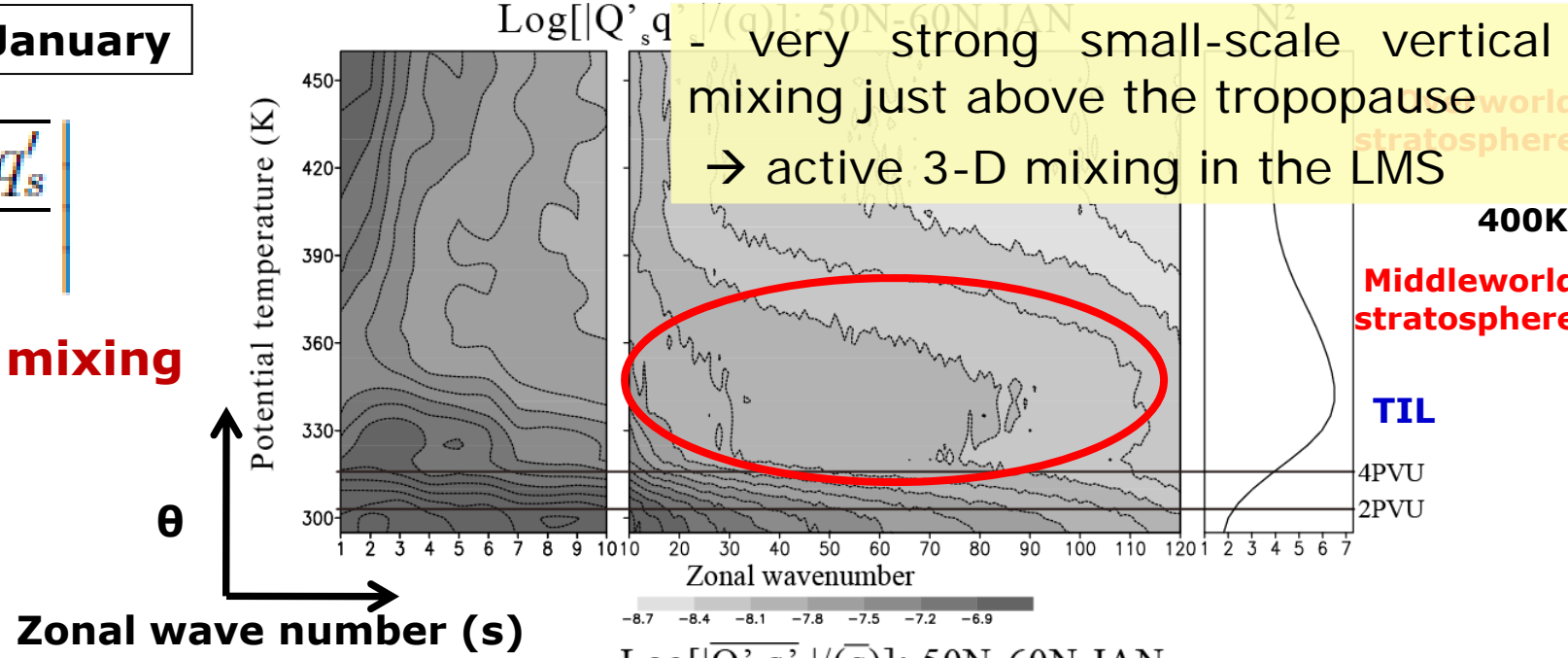
(m²s⁻¹)

(%)

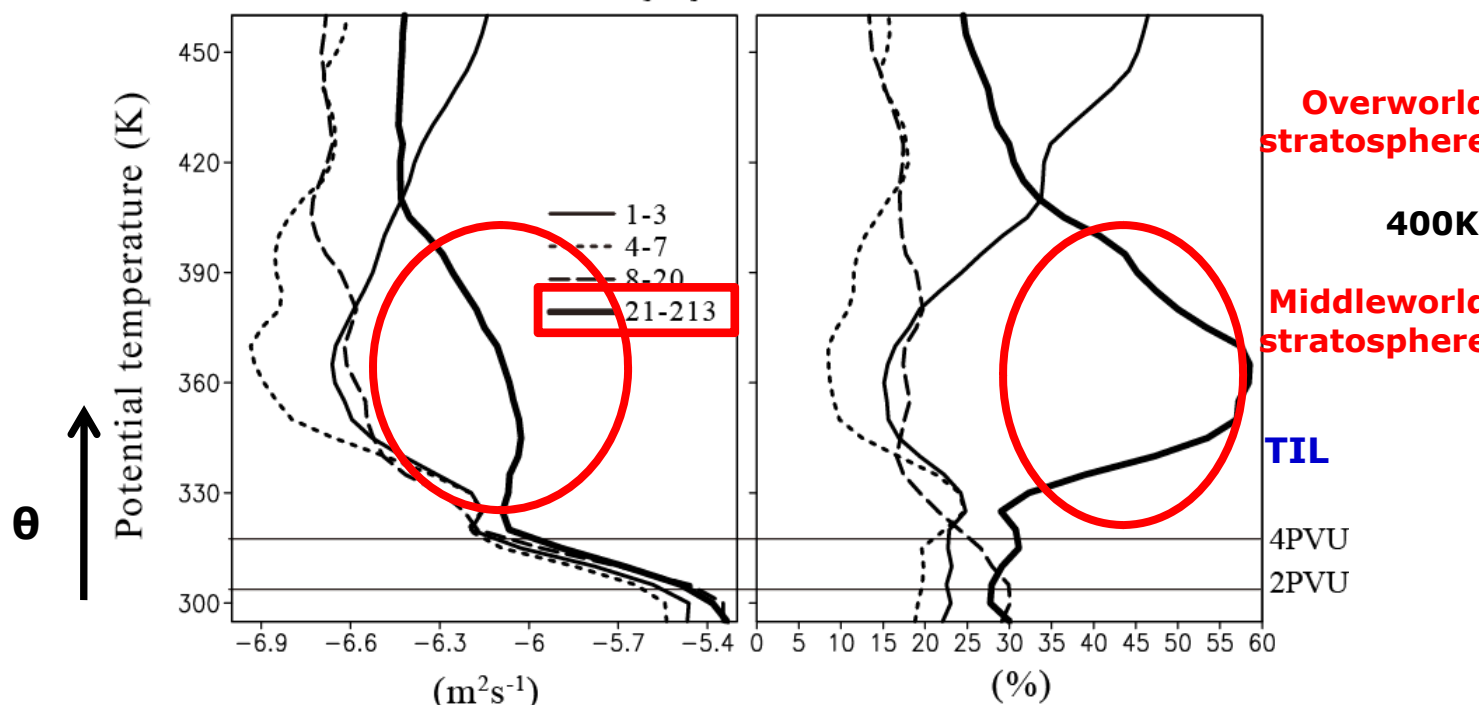
50N-60N January

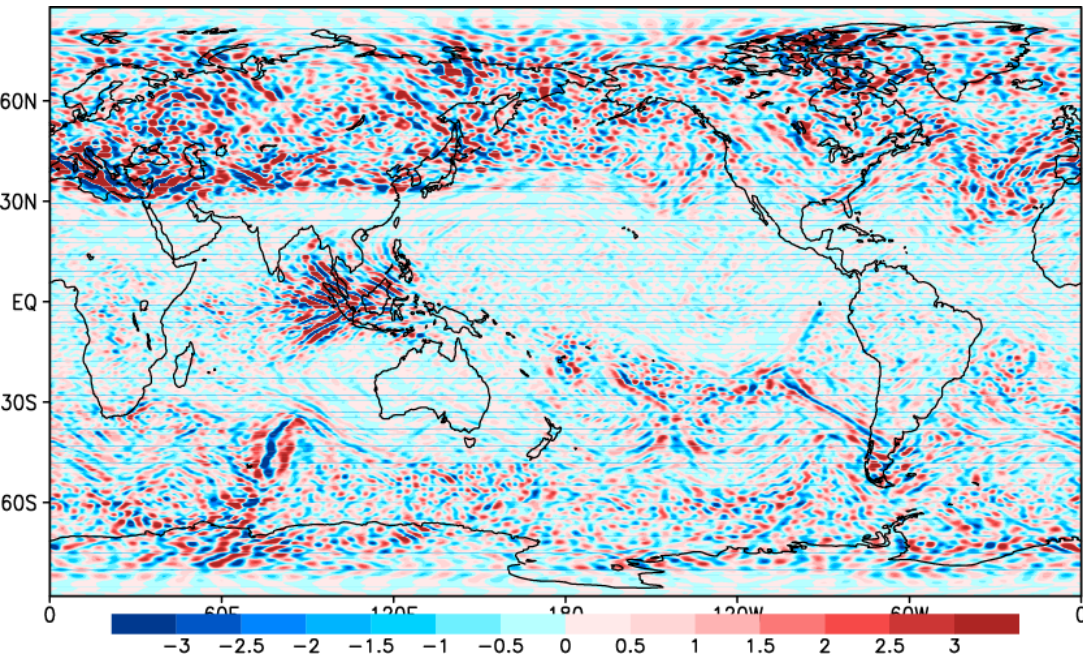
$$\left| \frac{Q'_s q'_s}{\bar{q}} \right|$$

Vertical mixing



Log[|Q'_s q'_s| / (q̄)]: 50N-60N JAN

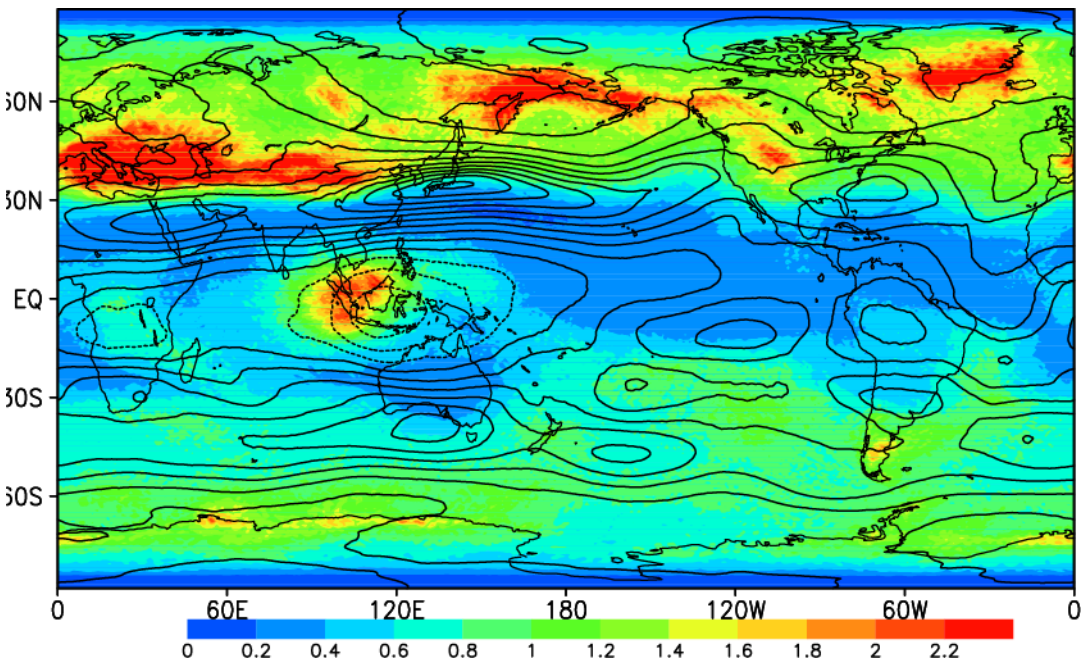




PV' for $n > 21$ at 360K

← **Snap-shot picture**

The small-scale disturbances occur over possible sources of gravity waves (mountains, cyclones, fronts, convection)



-> The propagation and breaking of gravity waves activate 3-D mixing in the TTL.

January

← **Monthly mean amplitude**

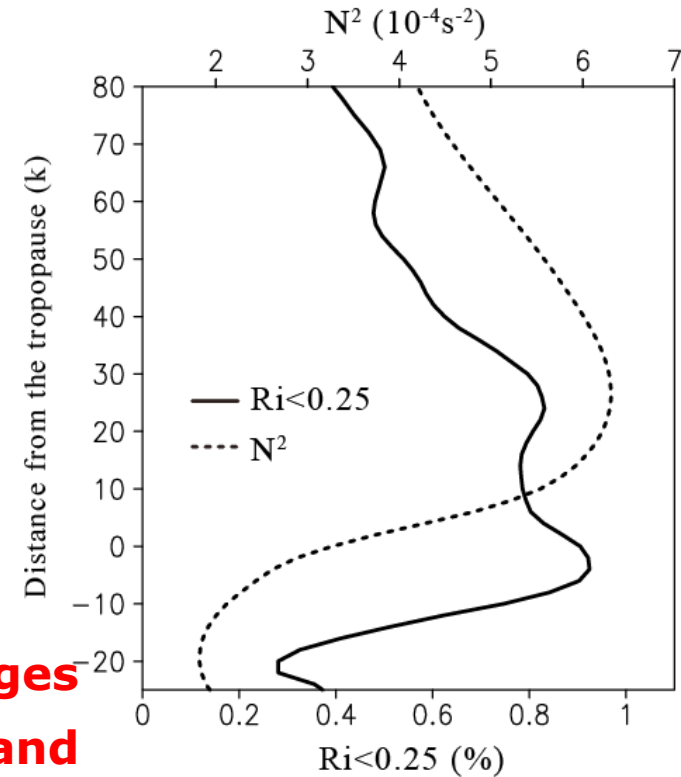
Discussions: GWs and small-scale mixing around the TIL

- The linear wave theory: a large static stability allows the occurrence of large-amplitude GWs due to increase of the saturation amplitude.
- Even when GWs do not break, large-amplitude GWs can be dissipated due to radiative relaxation and can cause eddy vertical dispersions (under non-uniform diabatic heating fields).

- Just above the TIL, GWs can easily reach their saturation limit and breaking level because of a rapid decrease in static stability (and ρ) with height.

- Dynamic instability occurs more frequently in the tropopause region than at other levels, which also may lead to the saturation.

- These situations associated with rapid changes in static stability and the dissipation and saturation of GWs can cause small-scale 3-D mixing around the TIL.



N² & Probability of the occurrence of Ri < 0.25

- The ExTL arises from downward transports in the lower levels and isentropic (winter) and vertical (summer) mixing in the upper levels.
- The TIL and the ExTL can be collocated because of common transport processes for constituents and heat and interactions between them.
- The small-scale dynamics associated with GWs play important roles in driving tracer transports. It is important to include these effects in GCMs or CTMs to obtain better simulations of the TIL and ExTL.

